Comunicações Geológicas

Comunicações Geológicas (2025) 112, Especial I, 197-200
ISSN: 0873-948X; **e-ISSN**: 1647-581X

Evaluation of pXRF as an exploration tool in soil analysis to detect antimony mineralizations: Case study in Ribeiro da Serra and Tapada - Northern Portugal

Avaliação do pXRF como ferramenta de prospeção em análises de solo para deteção de mineralizações de antimónio: Caso de estudo em Ribeiro da Serra e Tapada- Norte de Portugal

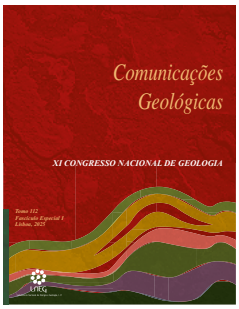

M. Carvalho[1, 2*], G. Resta[1, 2], A. Carvalho[1, 2], R. Frutuoso[2], A. Lima[1, 2]

DOI: https://doi.org/10.34637/x3f3-sv98

Recebido em 30/09/2023 / Aceite em 26/03/2024

Publicado online em abril de 2025

Artigo original
Original article

Abstract: A portable X-ray fluorescence (pXRF) is a tool that enables qualitative and semi-quantitative elemental analysis in real-time. In this study, the accuracy of the method for the quantitative analysis of antimony in the ancient mining areas of Ribeiro da Serra and Tapada was evaluated using soil samples. The obtained results were favourable regarding the ability to identify and quantify antimony (Sb) in soil samples without prior preparation.

Keywords: Portable X-Ray Fluorescence, antimony mineralization, soil analysis, Ribeiro da Serra, Tapada

Resumo: Fluorescência de Raios-X portátil (pXRF) é uma ferramenta que possibilita análises elementares qualitativas e semi-quantitativas em tempo real. Neste trabalho foi avaliada a exatidão do método para a análise quantitativa de antimónio nas antigas zonas mineiras de Ribeiro da Serra e Tapada, utilizando amostras de solo. Os resultados obtidos foram favoráveis quanto à capacidade de identificação e quantificação do antimónio (Sb) em amostras de solo sem preparação prévia.

Palavras-chave: Fluorescência de raios-X, mineralizações de antimónio, análise de solos, Ribeiro da Serra, Tapada

[1] Departamento de Geociências, Ambiente e Ordenamento do Território, Faculdade de Ciências, Universidade do Porto, rua do Campo Alegre s/n, Porto 4169-007, Portugal.

[2] Instituto de Ciências da Terra, Pólo Porto, rua do Campo Alegre 687, Porto 4169-007, Portugal.

[*] Autor correspondente / Corresponding author: morgana.carvalho@fc.up.pt

1. Introduction

Portable X-ray Fluorescence (pXRF) analysis in exploration offers cost reduction and streamlines sample preparation compared to other analytical methods. In addition, it enables real-time evaluation of results during fieldwork.

In this study, pXRF was tested as an exploration tool with the minimum preparation of the raw samples. The study was conducted in the encompassing zone of Ribeiro da Serra and Tapada, two abandoned mining complexes from the late 19th century where antimony was exploited.

2. Geological setting

The former Sb-Au mining concessions of Ribeiro da Serra and Tapada, are situated in Gondomar municipality, approximately 15 km from the city of Porto, at Serra das Flores. These deposits are located in the Iberian Massif, within a Proterozoic and/or Palaeozoic unit that constitutes the western side of the Central Iberian Zone. The antimony deposits are within the western flank of the Valongo anticline, in the Dúrico-Beirão Mining District (Figura 1).

Sb-Au mineralisations are mainly concentrated on the inverse flank, between Covelo and Sobrido regions. Sb-Au deposits are hosted by metasedimentary rocks from the Cambrian/Precambrian Schist-Greywacke Complex (ante-Ordovician), and breccias from the lower Carboniferous (Couto, 1993). From West to East, the lithologies in the study area range from ante-Ordovician schists and greywackes to lower Carboniferous breccias, conglomerates, quartzites, black schists and lydites, as well as Ordovician schists with some quartzites.

Carvalho (1969) referred that veins within the Schist-Greywacke Complex, primarily composed of schists, constitute the Au-Sb deposits. These deposits, characterized by low-volume Sb content, are sporadic and possess a hydrothermal origin attributed to the Hercynian granites. The dominant directions of the country rocks go from N to NW dipping to W. The most productive veins occur in the E-W direction, dipping to N (Tapada) and N-S dipping to W (Ribeiro da Serra). Ferreira (1970) reports that the Sb is present as stibnite, berthierite, and their alteration oxides and hydroxides phases. In addition, pyrite, antimony sulfosalt, silver (pyrargyrite?), gold, and quartz are other minerals in the zone.

3. Mines history

Both former concessions produced ~1 200 T of antimony and 2 T of gold, partially recovered (Couto *et al*., 1990). Kernow Mining Portugal (2009) refer that in the anticlinal region, the exploration of veins in the mines occurred until 100-200 m of depth in Ribeiro da Serra and 270 m in Tapada, and it is possible to see old galleries and wastepiles from their explotation from both. Carvalho (1969) revealed that, in 1858, Sb exploration started at a good pace in Ribeiro da Serra and Tapada. However, the entrance of Asian countries into the market may have caused a world crisis in the exploration of Sb, which lead to these mines closing around 1890.

4. Material and methods

Soil sampling campaigns

A soil sampling campaign was performed using a 50x50 m grid over the target areas. The direction of the soil profiles took into consideration the regional strike of the Douro Shear Zone, the Valongo anticline, and the perpendicular to the exploited veins rich in Sb-Au. The soil

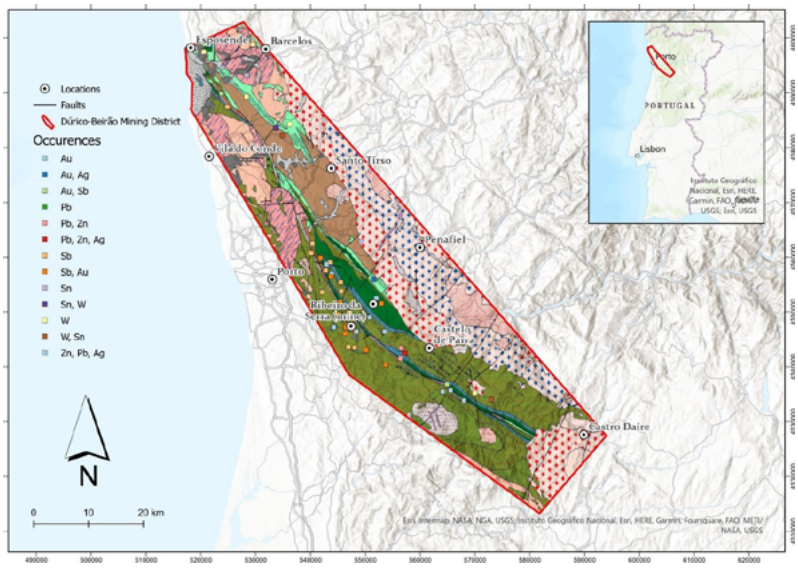

Figure 1. Dúrico-Beirão mining district Geological Map of Portugal (1:50 000) and relevant metallic occurrences (Modified after Serviços Geológicos, 1963). Coordinates in UTM 29N.

Figura 1. Mapa geológico do distrito mineiro Dúrico-Beirão de Portugal (1:50 000) e ocorrências metálicas relevantes (Modificado de Serviços Geológicos, 1963). Coordenadas em UTM 29N.

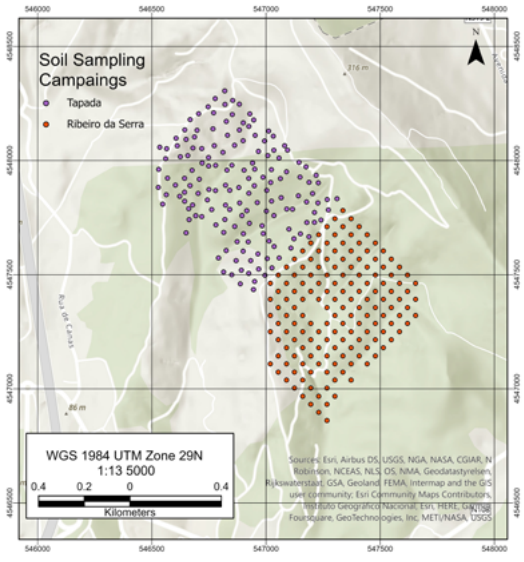

Figure 2. Location of collected soil samples for Ribeiro da Serra and Tapada.

Figura 2. Localização das amostras de solo recolhidas para Ribeiro da Serra e Tapada.

samples were collected preferentially from soil horizon B. Rainy days and wet soils were avoided. In total, 309 samples were collected, 157 from Ribeiro da Serra and 152 from Tapada (Figura2).

4.1. pXRF analysis

The pXRF instrument used in this study was the Bruker S1 Titan X-ray fluorescence analyser in the analysis's mode was GEOexploration. We directly analysed the samples from the collection bags (polyethylene bags) with the equipment and used a 90 second beam with 30 seconds by phase to analyse each soil sample in three different portions. Three measurements were obtained for each point and them the average was calculated.

4.2. ICP-MS analysis

From the totality of samples, 54 samples from Ribeiro da Serra and 53 samples from Tapada were selected to be analysed in an accredited laboratory (Bureau Veritas) by Inductively Coupled Plasma Mass Spectrometry (ICP-MS) analysis. The samples were previously milled to less than 200 µm in an agate mortar. The preparation for the analyses involved drying the selected samples in a dryer, in a temperature of 55 °C for at least 48 hours. They were quartered and 1/8 of the sample was ground in a mechanical agate mill for 10 minutes. Later, the samples were manually grinded in a mortar with a pestle, until all the contents passed through a 200 µm sieve.

The ICP-MS method comprises multi-acid digestion to give near total values for most elements. Is heated 0.25 g split in HNO_3, $HClO_4$ and HF to fuming and taken to dryness. The quality control method involves certified reference materials (OREAS45H, OREAS501D, OREAS25A-4A), blanks and random duplicates.

4.3. Combined Standard Uncertainty

The evaluation of the pXRF results was made considering the uncertainty associated with the pXRF analyser, the combined standard uncertainty, uc, was calculated using equation 1, where SD is the standard deviation of the repeated measurements and u_{FP} is the maximum uncertainty reported by the manufacture's $_{FP}$ algorithm (Guimarães *et al*., 2016).

To obtain evaluation metrics such as the Root Mean Squared Error (RMSE) and coefficient of determination (R^2) for comparing the pXRF results with the ICP-MS results, the calculation was implemented in Python. The comparison between the Factor Loads obtained by R-mode Factor Analysis (Klovan, 1975) and the PCA (principal component analysis) Scores is also employed to evaluate the results obtained (Lemière *et al*., 2020).

The PCA Scores were obtained using the scikit-learn library

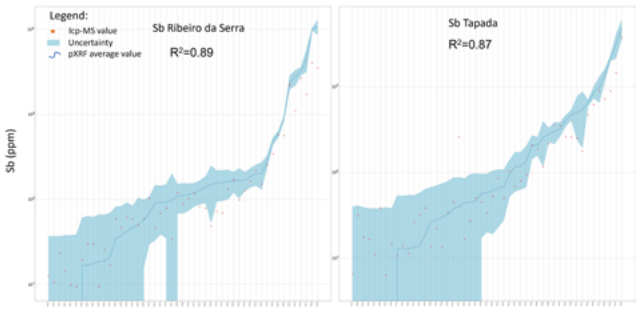

Figure 3. pXRF and ICP-MS values for Sb along with the uncertainty plot. The x-axis represents the samples in ascending order based on the Sb values obtained from ICP-MS analysis. The blue line represents the average value measured by pXRF, while the shaded area illustrates the associated uncertainty. The R^2 is obtained considering the uncertainty window. The y-axis represents the Sb values is in logarithmic scale to improve visualization.

Figura 3. Valores de pXRF e ICP-MS para Sb, juntamente com o gráfico de incerteza. O eixo x representa as amostras em ordem crescent, com base nos valores de Sb obtidos na análise ICP-MS. A linha azul representa o valor médio medido por pXRF, enquanto a área sombreada ilustra a incerteza associada. O R2 é obtido considerando a janela de incerteza. O eixo y representa os valores de Sb em escala logarítmica para melhorar a visualização.

Table 1. Descriptive Statistics for selected elements in Ribeiro da Serra
Tabela 1. Estatística Descritiva dos elementos selecionados no Ribeiro da Serra

RIBEIRO DA SERRA

	pXRF analysis (ppm)							ICP-MS analysis (ppm)						
	Sb	As	Ti	Pb	Mn	Zn	Fe	Sb	As	Ti	Pb	Mn	Zn	Fe
Mean	2160.46	183.31	0.3	88.23	72.8	26.28	36060.04	660.38	152.97	0.28	55.61	58.15	30.07	35161.11
Std. Deviation	5971.45	437.64	0.13	225.16	107.54	27.26	10888.2	1273.48	279.16	0.15	86	68.89	14.92	9739.15
Skewness	3.65	3.58	0.44	3.79	3.03	2.56	0.98	2.03	2.98	4	3.14	3.96	2.15	0.32
Std. Error of Skewness	0.32	0.32	0.32	0.32	0.32	0.32	0.32	0.32	0.32	0.32	0.32	0.32	0.32	0.32
Kurtosis	13.79	12.53	0.5	14.07	12.2	7.28	1.9	2.57	9.3	20.93	10.28	19.03	6.88	0.73
Std. Error of Kurtosis	0.64	0.64	0.64	0.64	0.64	0.64	0.64	0.64	0.64	0.64	0.64	0.64	0.64	0.64
Minimum	0	11.67	0.05	3.67	0	6.33	15390.67	9.5	14.8	0.13	12.26	9	11.1	11500
Maximum	31247.33	2152	0.68	1113.67	616.33	148	73976	4001	1431.2	1.14	449.03	442	95.3	62800

Table 2. Descriptive Statistics for selected elements in the Tapada Zone
Tabela 2. Estatísticas Descritivas dos elementos selecionados na Zona da Tapada

TAPADA

	pXRF analysis (ppm)							ICP-MS analysis (ppm)						
	Sb	As	Ti	Pb	Mn	Zn	Fe	Sb	As	Ti	Pb	Mn	Zn	Fe
Mean	519.17	47.94	2777.34	26.95	86	24.52	34702.14	394.62	103.23	3339.43	55.37	112.94	44.85	39466.04
Std. Deviation	2822.02	124.68	1188.79	97.76	188.15	15.89	11137.25	917.02	194.32	1815.28	146.13	164.01	26.85	10470.91
Skewness	10.26	9.12	1.11	11.06	4.21	2.8	0.2	3.44	4.23	3.47	6.25	3.19	1.91	0.96
Std. Error of Skewness	0.2	0.2	0.2	0.2	0.2	0.2	0.2	0.33	0.33	0.33	0.33	0.33	0.33	0.33
Kurtosis	113.76	94.36	5.74	129.57	20.46	10.97	-0.02	11.24	20.77	13.96	41.61	11.21	4.38	2.98
Std. Error of Kurtosis	0.39	0.39	0.39	0.39	0.39	0.39	0.39	0.64	0.64	0.64	0.64	0.64	0.64	0.64
Minimum	0	6	138	0	0	3.33	3818.33	6.3	16.4	1450	9.26	13	17.8	20000
Maximum	32716.67	1403.67	9515.67	1181.33	1328	115.67	68743	4001	1208.1	12000	1040.14	844	146	79300

Table 3. Evaluation of the results obtained by pXRF compared to ICP-MS results.
Tabela 3. Avaliação dos resultados obtidos por pXRF comparados com os resultados do ICP-MS.

RIBEIRO DA SERRA

	R2	RMSE	RMSE (0- 50 ppm)	RMSE (50- 100 ppm)	RMSE (100- 1000 ppm)	RMSE (>1000ppm)
Sb	0.89	164.65	0.00	0.00	68.22	502.85
As	0.38	225.61	10.20	19.99	330.35	1150.12
Ti	0.73	0.11	-	-	-	0.11
Pb	-0.03	95.83	10.99	10.07	112.31	407.13
Zn	0.24	19.40	13.59	37.49	44.63	-
Mn	0.52	47.98	5.63	13.90	93.30	-
Fe	0.98	0.40	-	-	-	0.40

TAPADA

	R2	RMSE	RMSE (0- 50 ppm)	RMSE (50- 100 ppm)	RMSE (100- 1000 ppm)	RMSE (>1000ppm)
Sb	0.87	54.82	0.11	64.40	38.92	124.61
As	0.89	65.67	4.99	8.50	53.26	-
Ti	0.13	0.13	-	-	-	0.13
Pb	0.99	9.41	9.15	7.28	-	-
Zn	0.75	0.87	14.80	34.72	-	-
Mn	0.95	37.84	5.83	-	73.76	-
Fe	0.98	0.48	-	-	-	0.48

(Pedregosa *et al.*, 2011) in a Python script, and the Factor Scores were obtained using the factor_analyzer Python module. Before obtaining the Factor Scores the adequacy of the data was evaluated by Bartlett's test of sphericity and by the Kaiser-Meyer-Olkin Test. The number of factors was chosen to consider the eigenvalues with values greater than one. This analysis also was performed using a Python script.

5. Results

The descriptive statistics for the selected elements, obtained for Ribeiro da Serra and Tapada by pXRF and ICP-MS are presented in the Table 1 and Table 2.

Considering the uncertainty, R^2 and RMSE for different concentrations of the elements were obtained by comparing the pXRF results with the results obtained by ICP-MS analysis (Table 3).

Figure 3 shows the pXRF measurements for Sb, compared with the ICP-MS values and the uncertainty. The results for the PCA analysis are in the Table 4 and the results for the Factor analysis are in Table 5.

In the context of the study, R^2 is used to evaluate the accuracy of the pXRF measurements compared to the ICP-MS results. When compared with the samples analyzed by ICP-MS, antimony exhibits a R^2 of 0.89 for the Ribeiro da Serra samples and 0.87 for the Tapada samples. It's important to notice that some elements, such as As, Pb, Zn, and Mn show significantly different R^2 for the measurements from Ribeira da Serra and Tapada. In the case of As and Pb it happens because Ribeira da Serra has higher concentrations for those elements, and the pXRF accuracy lowers as the concentration of those elements increases. It is expressed in the higher values of RMSE observed for concentrations of As and Pb that are higher than 1000 ppm. It is also worth remarking that, when the values are very low, they may have a good R^2 in consequence of a relatively high value of uncertainty.

The Factor analysis and PCA help investigate the association of elements. They allow us to perceive if the association between the

Table 4 - Evaluation of the PCA loads obtained by pXRF compared to ICP-MS results.

Tabela 4 - Avaliação das cargas de PCA obtidas por pXRF em comparação com resultados de ICP-MS.

Ribeiro da Serra						Tapada					
XRF			ICP-MS			XRF			ICP-MS		
	PC1	PC2		PC1	PC2		PC1	PC2		PC1	PC2
Fe	0.21	-0.61	Fe	0.72	0.00	Fe	0.36	0.73	Fe	0.47	0.64
Sb	0.68	0.64	Sb	0.77	-0.38	Sb	0.95	-0.28	Sb	0.78	-0.46
As	0.82	0.48	As	0.78	-0.10	As	0.94	-0.26	As	0.81	-0.49
Ti	-0.45	-0.25	Ti	0.10	0.88	Ti	-0.07	0.76	Ti	0.12	0.71
Pb	0.91	-0.14	Pb	0.83	-0.28	Pb	0.95	-0.25	Pb	0.79	-0.51
Mn	0.85	-0.36	Mn	0.84	0.31	Mn	0.27	0.72	Mn	0.57	0.66
Zn	0.82	-0.46	Zn	0.73	0.36	Zn	0.64	0.53	Zn	0.72	0.56

Table 5- Evaluation of the Factor scores obtained by pXRF compared to ICP-MS results.

Tabela 5- Avaliação das pontuações fatoriais obtidas por pXRF em comparação com os resultados do ICP-MS.

Ribeiro da Serra						Tapada					
XRF			ICP-MS			XRF			ICP-MS		
	F1	F2		F1	F2		F1	F2		F1	F2
Sb	0.98	-0.04	Sb	0.93	-0.11	Sb	1.00	0.03	Sb	0.84	0.05
As	0.95	0.18	As	0.73	0.16	As	0.97	0.05	As	0.95	0.03
Ti	-0.33	-0.16	Ti	-0.08	0.34	Ti	-0.23	0.56	Ti	-0.22	0.51
Pb	0.55	0.68	Pb	0.80	0.18	Pb	0.98	0.06	Pb	0.93	0.02
Zn	0.26	0.94	Zn	0.43	0.67	Zn	0.39	0.67	Zn	0.27	0.90
Mn	0.35	0.86	Mn	0.58	0.74	Mn	0.03	0.66	Mn	0.09	0.83
Fe	-0.06	0.30	Fe	0.54	0.34	Fe	0.11	0.72	Fe	0.03	0.66

elements remains with the variation in the measurements. For the factor analysis (Table 5), we see that for Ribeiro da Serra, Pb (the element with the worst R^2), belongs to a different factor when the two analyses are compared. For Tapada, the elements exhibit slightly different loads but remain in the same factors.

The PCA analysis (Table 4) resulted in components that show different associations between elements than those seen in the factor analysis. We see there are variations in the components for Ribeiro da Serra, and for Tapada the association between elements remains the same and reflects what was found in the factor analysis.

6. Discussion

For the elements highlighted in this study, pXRF has shown limitations in providing accurate values when high contents of As and Pb are present in the soil samples, as observed in Ribeiro da Serra.

Compared with the samples that were sent to the ICP-MS analysis, antimony shows an R^2 of 0.9 for the Ribeiro da Serra samples and 0.88 for the Tapada samples, which demonstrates that the tool can provide fast and effective quantification for this element.

The associations between Sb and other elements, obtained by Factor Analysis loads and PCA scores, can vary depending on the accuracy of the pXRF measurements. We noticed that, in the case of Ribeiro da Serra by applying factor analysis and PCA to the data obtained from different analyses, we find different associations between elements, that could lead to different interpretations.

How much the uncertainty varies in an interval is an important aspect to be considered when using pXRF measurements to evaluate low concentrations of elements, such as concentrations that can indicate contaminations. In a scenario where a statistical analysis will be conducted, it is worth evaluating what level of uncertainty is acceptable. In scenarios when the time frame allows, it may be interesting to consider additional steps for the sampling preparation, as preparation of pressed pellets, grinding and others (Goff *et al*., 2020) can mitigate this problem.

7. Conclusions

The evaluation of the pXRF proves its efficiency in the exploration of Sb, being useful for testing the mineralization distribution and identifying possible new mineralized structures, providing fast and satisfactory results with no need for previous preparation of the samples. However, to use correlations of geochemical data between values of several elements obtained by pXRF, it is important to consider that the results may not be accurate for certain elements. Considering the uncertainty associated with the pXRF measurements, it helps evaluating which intervals of Sb measurements could indicate potential mineralization or even soil contamination.

Acknowledgments

This work is supported by national funding awarded by FCT - Foundation for Science and Technology, I.P., projects UIDB/04683/2020 and UIDP/04683/2020.

The authors would like to acknowledge AUREOLE project MIN/0005/2018, DOI: 10.54499/ERA-MIN/0005/2018, for providing soil samples used in this study.

References

Carvalho, A. D. de., 1969. Minas de Antimónio e Ouro de Gondomar. *Estudos, Notas e Trabalhos*, **19**: 1-2.

Couto, H., 1993. As mineralizações de Sb-Au da região Dúrico-Beirã. Faculdade de Ciências da Universidade do Porto.

Couto, H., Roger, G., Moëlo, Y., Bril, H., 1990. Le district à antimoine-or Dúrico-Beirão (Portugal): évolution paragénétique et géochimique; implications métallogéniques. *Mineralium Deposita*, **25**(S1): S69–S81. https://doi.org/10.1007/BF00205252

Ferreira, M. R. P. V., 1970. *Relatório sobre a Mina de Antimónio e Ouro de Alto do Sobrido*.

Goff, K., Schaetzl, R. J., Chakraborty, S., Weindorf, D. C., Kasmerchak, C., Bettis III, E. A., 2020. Impact of sample preparation methods for characterizing the geochemistry of soils and sediments by portable X-ray fluorescence. *Soil Science Society of America Journal*, **84**(1): 131-143.

Guimarães, D., Praamsma, M. L., Parsons, P. J., 2016. Evaluation of a new optic-enabled portable XRF instrument for measuring toxic metals/metalloids in consumer goods and cultural products. *Spectrochimica acta*. Part B, *Atomic spectroscopy*, **122**: 192.

Kernow Mining Portugal, 2009. *Sobrido - 5° Relatório de Actividades*. Kernow Mining Portugal

Klovan, J. E., 1975. R- and Q-Mode Factor Analysis. In: McCammon, R. B. (Ed.), *Concepts in Geostatistics*. Springer, Berlin, Heidelberg. https://doi.org/10.1007/978-3-642-85976-2_2.

Lemière, B., Melleton, J., Auger, P., Derycke, V., Gloaguen, E., Bouat, L., Mikšová, D., Filzmoser, P., Middleton, M., 2020. pXRF measurements on soil samples for the exploration of an antimony deposit: Example from the Vendean Antimony District (France). *Minerals*, **10**(8): 724.

Serviços Geológicos, 1963. *Carta Geológica de Portugal - 13-B (1:50 000)*. https://geoportal.lneg.pt/mapa/?mapa=CGP500k.

Pedregosa, F., 2011. Scikit-learn: Machine learning in python Fabian. *Journal of machine learning research*, **12**: 2825.